DTP/96/22
RAL-TR-96-019
March 1996

Can partons describe the CDF jet data?

E. W. N. Glover[a], A. D. Martin[a], R. G. Roberts[b] and W. J. Stirling[a,c]

[a] *Department of Physics, University of Durham, Durham, DH1 3LE*
[b] *Rutherford Appleton Laboratory, Chilton, Didcot, Oxon, OX11 0QX*
[c] *Department of Mathematical Sciences, University of Durham, Durham, DH1 3LE*

Abstract

The recent CDF single jet inclusive measurements at Fermilab are incorporated in a global next-to-leading order parton analysis of the available deep inelastic and related data. We find that it is impossible to achieve a simultaneous QCD description of both the CDF jet distribution for transverse energies $E_T > 200$ GeV and the deep inelastic structure function data for $x > 0.3$. However, the CDF data for $E_T < 200$ GeV and the deep inelastic data are adequately described provided that the QCD coupling $\alpha_S(M_Z^2)$ is increased from its preferred deep inelastic value to $\alpha_S(M_Z^2) \simeq 0.116 - 0.120$.

The measurement of the differential cross section for inclusive central jet production at the Fermilab $p\overline{p}$ collider has recently been reported by the CDF collaboration [1] for jet transverse energies, E_T, in the range 15 to 440 GeV. At the higher E_T values these measurements probe the substructure of the proton in a previously unexplored kinematic region, equivalent to 4-momentum transfer squared $Q^2 \sim 10^5$ GeV^2 which corresponds to distance scales of $O(10^{-17}$ m) or less. Intriguingly, the experimental results for $E_T > 200$ GeV show evidence of a possible deviation above the behaviour predicted by next-to-leading order (NLO) QCD based on the current sets of parton distributions — distributions which are obtained from global analyses [2, 3, 4] of a wide range of deep inelastic and related data. Clearly before explanations based on New Physics [5] can be taken seriously, it is crucial to see if the parton distributions can be adjusted to accommodate the jet measurements whilst retaining a satisfactory description of the other data. Here we address this vital question.

We begin by comparing the CDF jet measurements with the (NLO) prediction obtained from the MRS(A$'$) set of partons [4] which, at present, seem best able to describe all the other data. The calculation uses the next-to-leading-order parton level Monte Carlo JETRAD [6] and the cuts and jet algorithm applied directly to the partons are modelled as closely as possible to the experimental set-up. The jets are defined according to the Snowmass algorithm with a jet cone size $R = 0.7$ [7], and are required to lie in the pseudo-rapidity range between $0.1 < |\eta| < 0.7$. The factorization and renormalization scales are chosen to be $\mu_F = \mu_R = E_T/2$. The fractional difference between data and theory is given by comparing the data points with the horizontal line in Fig. 1.[1] Over the observed range of E_T the experimental cross section falls by more than 8 orders of magnitude and the sum of the *correlated* systematic uncertainties grows from $\pm$ 18% at $E_T = 50$ GeV to $\pm$ 28% at $E_T = 300$ GeV. However, the statistical precision of the data is such that the difference between the observed and predicted shapes of the E_T distribution must be studied seriously. Although we have selected MRS(A$'$), it is important to note that the comparison is very similar for the other parton sets obtained from global analyses which include both fixed-target and HERA deep inelastic data, see Fig. 1 of Ref. [1]. Disregarding a small change in normalization, the nature of the discrepancy between the MRS(A$'$)-based prediction and the data differs according to whether the jet E_T is below or above about 200 GeV. Interestingly it is around this value that jet production changes from being dominated by qg-initiated to (valence quark) $q\overline{q}$-initiated QCD subprocesses, see Fig. 2.

Before we present a global parton analysis which incorporates both the deep inelastic and jet data we discuss some general trends that can already be established, bearing in mind that a centrally produced jet of transverse energy E_T samples partons at

$$x \;\sim\; 2E_T/\sqrt{s}, \qquad Q^2 \;\sim\; E_T^2 \tag{1}$$

where $\sqrt{s} = 1.8$ TeV at the Tevatron collider. First we note that the discrepancy in the shape of the jet distribution for $E_T < 200$ GeV could be removed either by significantly increasing the

[1] For clarity we have not made the small overall renormalization of the A$'$ prediction which would improve the average absolute value, but not the description of the *shape* of the jet distribution.

QCD coupling from the MRS(A′) value of $\alpha_S(M_Z^2) = 0.113$ (see Refs. [8, 9]) or by increasing the gluon in the $x \sim 0.1$ region (see, for example, the MRS(D_0') [10] "base" line in Fig. 1 of Ref. [1]). Both options lead to disagreement with data elsewhere. The effect of increasing α_S is to increase the rate of increase in the partons at small x and to steepen the low E_T jet cross section as required, but it also leads to scaling violations of deep inelastic data which are too rapid. The second option is contrary to HERA data which require the gluon to be larger (and steeper) than D_0' for $x \leq 10^{-2}$ and hence, by momentum conservation, smaller (and steeper) for $x \sim 0.1$, see Fig. 15 of Ref. [2].

Turning now to the discrepancy for $E_T > 200$ GeV, we note that in this region the jet distribution depends on the partons (mainly the valence quarks, but also the gluon) with $x \sim 0.35 - 0.5$ and $Q^2 \sim 10^4 - 10^5$ GeV^2. The discrepancy has been accommodated in a recent analysis [11] by modifying the gluon distribution in this x region. Traditionally the gluon is constrained in the region $0.35 \lesssim x \lesssim 0.55$ by the WA70 prompt photon data [12]. In Ref. [11] it is argued that the modified gluon can be made consistent with the WA70 data by taking into account scale uncertainties and k_T broadening. However, increasing the gluon in this x range implies a decrease in the region $x \sim 0.01 - 0.3$ (see Fig. 2 of [11]) so the resulting partons do not describe the shape of the more precise jet data with $E_T < 200$ GeV, see the dotted curve in Fig. 1. Alternatively, it might appear that a judicious increase of the valence quark distributions by about 10% in the region $x \simeq 2E_T/\sqrt{s} \sim 0.35 - 0.45$ and $Q^2 \sim 10^4 - 10^5$ GeV^2 would remove the discrepancy for $E_T > 200$ GeV. However, these distributions are constrained, through GLAP evolution, by deep inelastic measurements at lower Q^2. In particular, precise large-x structure function data from BCDMS ($F_2^{\mu p}, F_2^{\mu d}$) [13], CCFR ($F_2^{\nu N}, xF_3^{\nu N}$) [14] and NMC ($F_2^{\mu n}/F_2^{\mu p}$) [15] pin down the dominant u and d distributions very accurately, see for example Ref. [2], with combined statistical and systematic errors of the order of a few percent. Data at smaller x also, through the effects of evolution and sum rules, constrain the structure functions at larger x. The situation is further complicated since an increase of the value α_S (which increases the jet subprocess cross section) tends, through evolution, to decrease the valence, and hence the jet, distributions at large Q^2.

It is clear that the jet data must be included in a global analysis to investigate whether a compromise overall fit can be achieved by adjusting the partons and $\alpha_S(M_Z^2)$, such that we have a satisfactory QCD description of the detailed shape of the entire jet spectrum without destroying the fit to the other data. We therefore perform a next-to-leading (NLO) analysis of the available deep-inelastic and related data as described in Ref. [2], but updated to include the published measurements of F_2 at HERA [16] together with the CDF jet data [1]. The inclusion of the HERA data impose an important constraint on the gluon at small x (and rule out, for example, partons such as MRS(D_0') [10] which were found to give an excellent prediction of the jet shape for $E_T < 200$ GeV). The HERA data pin down the quarks and gluons at small x and thus (through the sum rules) restrict their variation at larger x.

We fit to the shape of the jet data in the region $E_T > 50$ GeV where the NLO QCD description is, to a good approximation, scale independent (and where the experimental ambiguities

from the underlying event are small [1]). To implement an economical NLO description of the inclusive jet distribution within the global fit, we first calculate the K factor,

$$K \;=\; \frac{\sigma_{LO} \;+\; \sigma_{NLO}}{\sigma_{LO}} \tag{2}$$

as a function of E_T using MRS(A$'$) partons, but with larger $\alpha_S(M_Z^2) = 0.12$. The renormalization and factorization scales are set equal to $E_T/2$. A global analysis is performed in which the jet data are fitted to the distribution $K\sigma_{LO}$. The resulting optimum set of partons together with the corresponding value of $\alpha_S(M_Z^2)$ are then used to recompute the K factor, and the global fit repeated. This iterative procedure converges rapidly. For the above choice of scales the K factor is found, to a good approximation, to be independent of E_T in the interval $50 < E_T < 400$ GeV and equal to 1.10. The whole analysis is repeated taking the renormalization and factorization scales equal to E_T. It is found to yield essentially the same global fit, but the normalization of the jet data increases.

The new set of partons[2], which we denote by J, is found to have a significantly larger value of the QCD coupling, $\alpha_S(M_Z^2) = 0.120$, as compared to 0.113 of MRS(A$'$), in order to give an improved description of the precise CDF jet data with $E_T < 200$ GeV, see Fig. 1. The improvement is obtained at the expense of a somewhat less satisfactory description of the scaling violations of the fixed-target deep-inelastic data. This is evident from the χ^2 values listed in Table 1. As an example, Fig. 3 shows the description of the large x BCDMS $F_2^{\mu p}$ deep inelastic data [13]. (A similar plot exists for the $F_2^{\mu d}$ and $F_2^{\nu N}, xF_3^{\nu N}$ data.) Note that there is in fact a continuum of such fits, spanned by A$'$ and J, in which $\alpha_s(M_Z^2)$ increases from 0.113 to 0.120 for which the fits to the deep-inelastic (low E_T jet data) gradually deteriorate (improve). In selecting fit J we are deliberately giving more weight in the fit to the CDF data.

The compromise fit, J, does not improve the description of the CDF jet data with $E_T > 200$ GeV. In fact we see from Fig. 1 that the fit is marginally inferior to A$'$. It turns out to be impossible to obtain a reasonable description simultaneously of the deep inelastic and CDF jet data over the full range of E_T. Because of their smaller errors the low E_T CDF data points have a bigger influence on the fit than those at large E_T. To illustrate the conflicting requirements of these data we successively omit deep inelastic data[3] starting from those at the largest x values until we can achieve a satisfactory description of the entire CDF jet E_T spectrum. We find that it is necessary to omit data with $x > 0.2$, that is a major fraction of the deep inelastic data, before a reasonable fit to the jet spectrum is obtained. The partons obtained in this way are denoted by J$'$. Although the fit to the jet E_T spectrum is satisfactory (see Fig. 1), these partons give a poor description of the omitted deep inelastic data — see, for example, the J$'$ prediction for the BCDMS data shown in Fig. 3.

In the J$'$ fit the quarks are drastically modified at large x compared to MRS(A$'$) in order to accommodate the large E_T CDF jet data. The question addressed in Ref. [11] is whether

[2]A similar fit, but with the jet data described by σ_{LO} was obtained in Ref. [17].

[3]However, we keep the NMC measurements [15] of F_2^n/F_2^p in the fit.

Expt.	# data	MRS(A′) χ^2	J χ^2	J′ χ^2
HERA F_2^p	206	115	96	95
BCDMS				
$F_2^{\mu p}$ $(x < 0.2)$	46	53	43	65
$F_2^{\mu p}$ $(x > 0.2)$	128	204	251	[20703]
CCFR				
$F_2^{\nu N}$ $(x < 0.2)$	29	60	74	74
$F_2^{\nu N}$ $(x > 0.2)$	51	35	32	[1290]
$xF_3^{\nu N}$ $(x < 0.2)$	29	18	19	18
$xF_3^{\nu N}$ $(x > 0.2)$	51	47	40	[896]
NMC				
$F_2^{\mu p}$ $(x < 0.2)$	29	77	74	70
$F_2^{\mu p}$ $(x > 0.2)$	55	36	41	[78]
$F_2^{\mu p}/F_2^{\mu n}$	85	137	136	131
CDF				
$d\sigma/dE_T$ $(E_T < 200$ GeV)	24	[158]	38	35
$d\sigma/dE_T$ $(E_T > 200$ GeV)	11	[14]	19	8
$\alpha_S(M_Z^2)$		0.113	0.120	0.129
CDF (renorm.)		[1.0]	1.04	1.21

Table 1: χ^2 values for various subsets of data; the values shown in square brackets correspond to data that are omitted from the fit.

the quarks can be kept essentially unchanged and the large E_T excess explained solely by a modified gluon density at large x. We have also performed fits of this type and find that the E_T distribution cannot be adequately described below and above $E_T \sim 200$ GeV simultaneously – in qualitative agreement with the conclusion one draws from the dotted curve [11] of Fig. 1. We have also explored the possibiliity of modifying the scale for α_S by including a factor $(1-x)/x$, which helps give the jet cross section a rise with increasing E_T. However, the resulting fit can produce qualitative agreement only over a very limited region ($E_T > 200$ GeV) provided a large renormalization of the jet data is made.

Fig. 4 compares the quark and gluon distributions, at $Q^2 = 10,\ 10^4$ GeV^2, of the new sets with those of MRS(A$'$). We plot the singlet quark distribution, $\sum_i (q_i + \bar{q}_i)$, since this is most closely related to the combination which is sampled by the jet cross section. Note that the area under the curves is the total momentum fraction carried by the quarks and gluons. We see that the main difference between the A$'$ and J distributions comes from the different value of α_S: the evolution between $Q^2 = 10$ GeV^2 and 10^4 GeV^2 is more pronounced for the J partons, such that at the latter scale the J quarks are respectively smaller and larger than the A$'$ quarks for $x \gtrsim 0.1$ and $x \lesssim 0.1$. This difference leads to a better fit to the small E_T CDF data, see Fig. 1. The starting gluons are very similar in the two sets. For both the A$'$ and J partons the overall renormalization required to give the best fit to the CDF jet data is well inside the experimental uncertainty. The J$'$ partons, on the other hand, have significantly harder quark distributions at large x, as anticipated from Figs. 1 and 3. At $Q^2 = 10^4$ GeV^2, the J$'$ quarks are larger than the A$'$ quarks for $x \gtrsim 0.35$ and $x \lesssim 0.08$, giving an improved fit to the CDF jet data both at large E_T *and* at small E_T. Notice also that the J$'$ gluon is significantly smaller than the A$'$ gluon at small x and $Q^2 = 10$ GeV^2. This is required in order to maintain a good fit to the HERA measurements of $\partial F_2/\partial \ln Q^2 \sim \alpha_S g$ with a significantly larger α_S.

In summary, we have attempted to incorporate the CDF inclusive jet cross section data in a global parton distribution analysis. We find that it is impossible to accommodate both the jet data *over the complete E_T range* and the deep inelastic structure function data.[4] However, the CDF data for $E_T < 200$ GeV and the deep inelastic data *can* be reasonably well fitted simultaneously. The main effect of including the jet data is to increase the value of α_S from the standard deep inelastic value. Interestingly, this slightly improves the fit to the HERA and low-x fixed target data. The fit to the large-x fixed data is however considerably worsened, see Table 1. The result of the combined fit is the J set of partons. It is impossible to simultaneously fit the large $E_T > 200$ GeV jet data. If one gives up the fit to the small E_T data, one can achieve a reasonble large E_T fit by adjusting the gluon distribution, as in the analysis of Ref. [11] for example. A fit over the whole jet E_T range (resulting in the J$'$ set of partons) yields quarks which are completely incompatible with the large-x structure function data, see

[4]This conclusion assumes that the systematic errors of the CDF data are strongly correlated and that the statistical errors define the *shape* of the distribution. It is relevant to note that for the UA2 inclusive jet data [18] there is no evidence for a discrepancy with the shape of the predicted NLO QCD distribution (i.e. a "break" in the region of $x_T \equiv 2E_T/\sqrt{s} \approx 0.25$), although in this case the large combined statistical and systematic errors may mask such structure; see Fig. 5 of Ref. [11].

Fig. 3, a value for α_S which is several standard deviations larger than the current world average, and a renormalization of the CDF jet data which is on the edge of the allowed range [1].

We therefore conclude that it is unlikely that the difference between the CDF inclusive jet cross section data and the standard NLO QCD prediction can be attributed to a deficiency in our knowledge of parton distributions.

Acknowledgements

We thank Al Goshaw and Anwar Bhatti for valuable discussions concerning the CDF data.

References

[1] CDF collaboration: F. Abe *et al.*, preprint Fermilab-PUB-96/020-E (1996).

[2] A.D. Martin, R.G. Roberts and W.J. Stirling, Phys. Rev. **D50** (1994) 6734.

[3] CTEQ collaboration: J. Botts *et al.*, Phys. Lett. **B304** (1993); H.L. Lai *et al.*, Phys. Rev. **D51** (1995) 4763.

[4] A.D. Martin, R G. Roberts and W.J. Stirling, Phys. Lett. **B354** (1995) 155.

[5] V. Barger, M.S. Berger and R.J.N. Phillips, Madison preprint MADPH-95-920 (1995).
G. Altarelli, N. Di Bartolomeo, F. Feruglio, R. Gatto and M. Mangano, CERN preprint CERN-TH-96-20 (1996).
P. Chiappetta, J. Layssac, F.M. Renard and C. Verzegnassi, Marseille preprint CPT-96-P-3304 (1996).
M. Bander, UC Irvine preprint UCI-TR-96-7 (1996).

[6] W.T. Giele, E.W.N. Glover and D.A. Kosower, Phys. Rev. Lett. **73** (1994) 2019.

[7] See, for example, J.E. Huth *et al.*, in Research Directions for the Decade, Proc. 1990 Divison of Particles and Fields Summer Study, Snowmass, 1990, ed. E.L. Berger (World Scientific, Singapore, 1992), p.134.

[8] W.T. Giele, E.W.N. Glover and J. Yu, Phys. Rev. **D53** (1996) 120.

[9] A.D. Martin, R.G. Roberts and W.J. Stirling, Phys. Lett. **B356** (1995) 89.

[10] A.D. Martin, R.G. Roberts and W.J. Stirling, Phys. Lett. **B306** (1993) 145.

[11] CTEQ collaboration: J. Huston *et al.*, Michigan State preprint MSU-HEP-50812 (1995).

[12] WA70 collaboration: M. Bonesini *et al.*, Z. Phys. **C38** (1988) 371.

[13] BCDMS collaboration: A.C. Benvenuti *et al.*, Phys. Lett. **B223** (1989) 485.

[14] CCFR collaboration: P.Z. Quintas *et al*, Phys. Rev. Lett. **71** (1993) 1307.

[15] NMC collaboration: P. Amaudruz *et al.*, preprint CERN-PPE/94-32.

[16] H1 collaboration: T. Ahmed *et al.*, Nucl. Phys. **439** (1995) 379; Talks at DIS 95 Workshop, Paris by J. Dainton and G. Raedel.
ZEUS collaboration: M. Derrick *et al.*, Zeit. Phys. **C65** (1995) 379 and DESY report 95-193 (1995).

[17] K.J. Stevenson, University of Durham, M.Sc. thesis, September 1995.

[18] UA2 collaboration: J. Alitti *et al.*, Phys. Lett. **B257** (1991) 232.

Figure Captions

Fig. 1 The fractional difference between the measured CDF inclusive jet cross section [1] and the NLO QCD predictions based on MRS(A′) [4], J and J′ parton sets. Also shown (by the dotted curve) is the gluon-modified description of Ref. [11]. The numbers shown in brackets are the renormalization factors used for the J and J′ partons. Only the statistical errors of the data are shown.

Fig. 2 The fraction of the leading-order jet cross section $d^2\sigma/dE_T d\eta|_{\eta=0}$ at the Tevatron originating from gg, qg and $q\overline{q}$ $(+qq)$ initiated QCD subprocesses using the MRS(A′) set of partons Ref. [4].

Fig. 3 The description of the large x BCDMS measurements of F_2^p by the MRS(A′) partons of Ref. [4], and the J and J′ partons of this work.

Fig. 4 The parton distributions g and $\sum_i(q_i + \bar{q}_i)$ at $Q^2 = 10$ and 10^4 GeV^2.

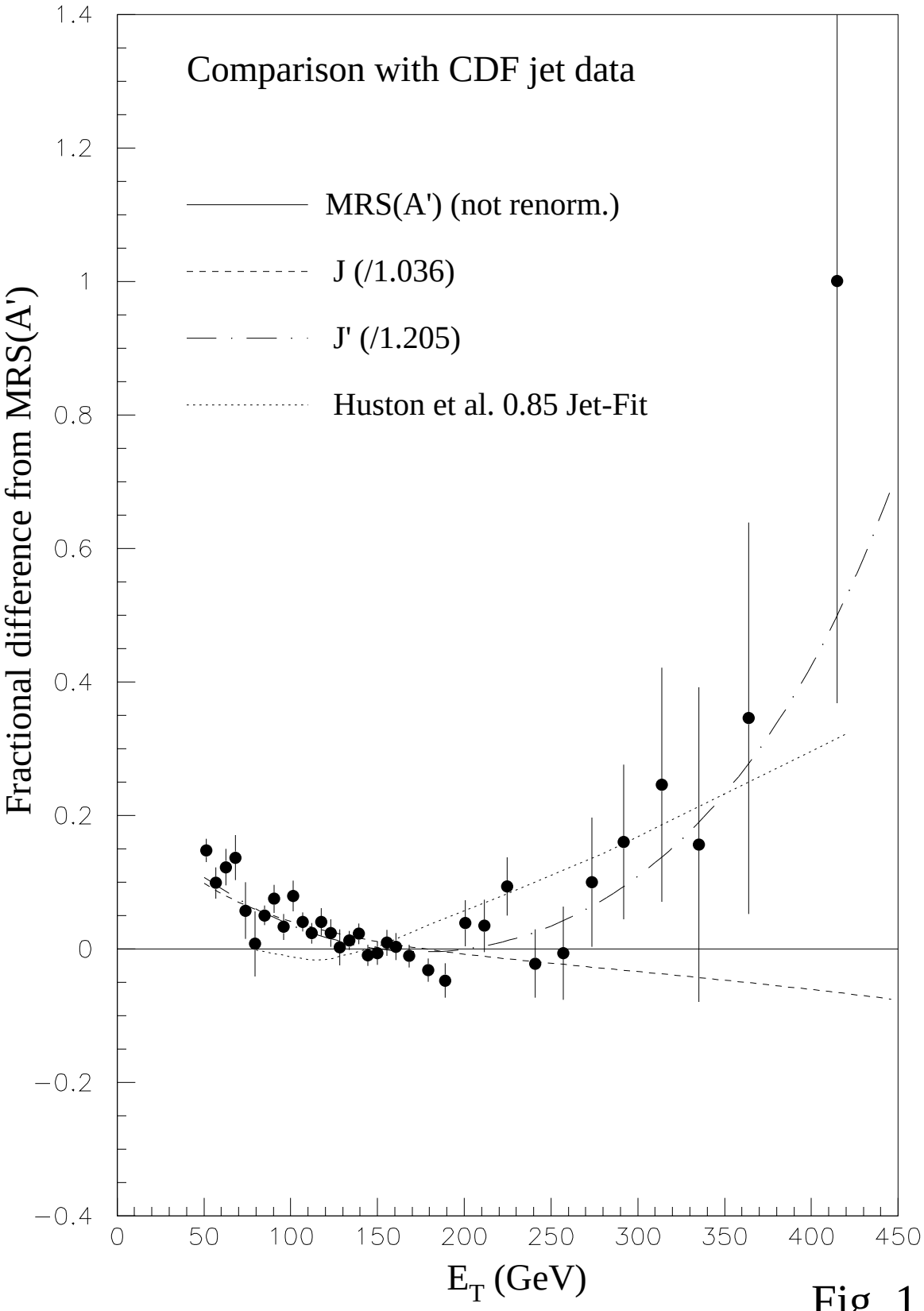
Comparison with CDF jet data
MRS(A') (not renorm.)
J (/1.036)
J' (/1.205)
Huston et al. 0.85 Jet-Fit
Fractional difference from MRS(A')
E_T (GeV)
1.4
1.2
1
0.8
0.6
0.4
0.2
0
−0.2
−0.4
0
50
100
150
200
250
300
350
400
450

Fig. 1

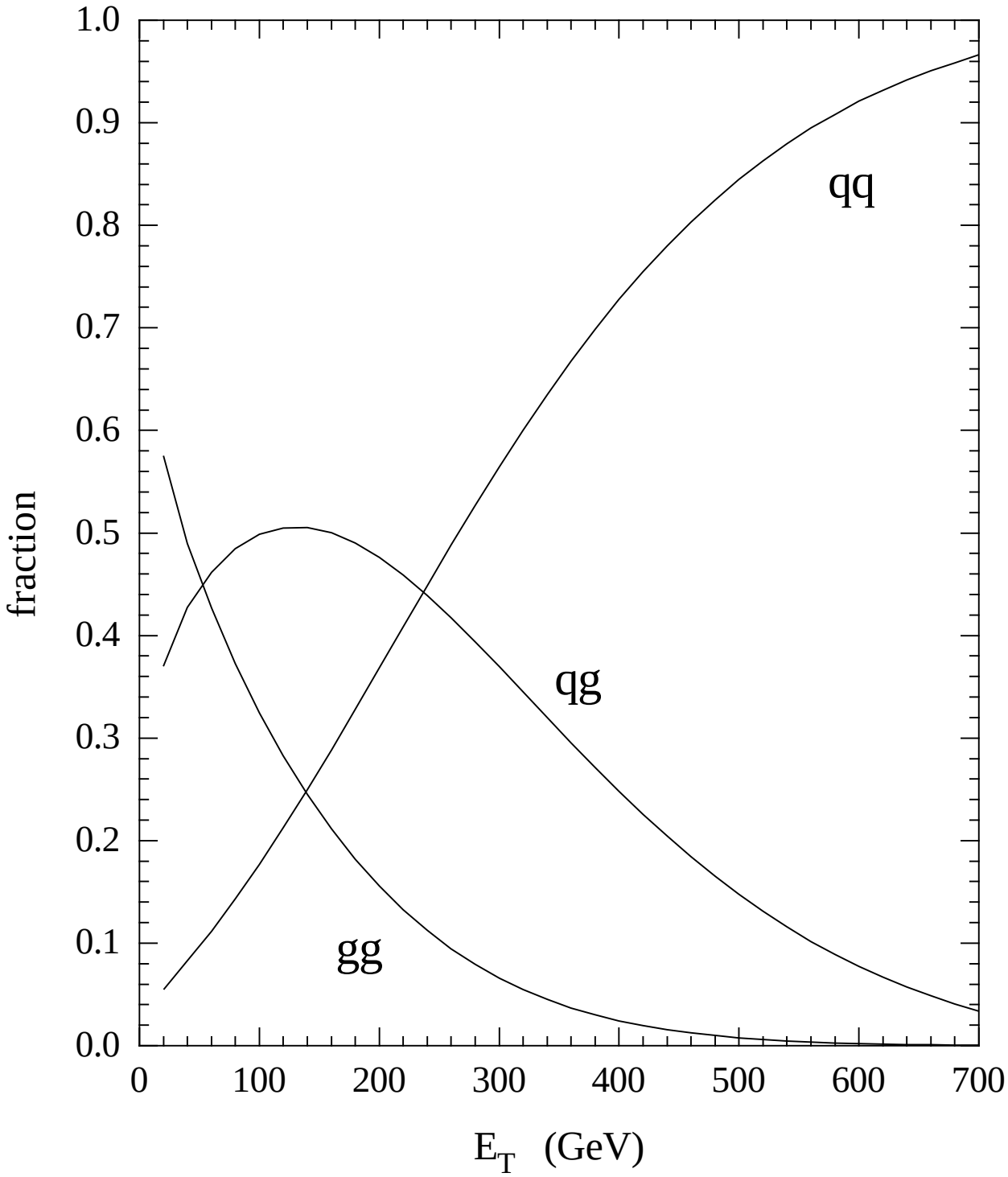
1.0
0.9
0.8
0.7
0.6
0.5
0.4
0.3
0.2
0.1
0.0
fraction
qq
qg
gg
0
100
200
300
400
500
600
700
E_T (GeV)

Fig. 2

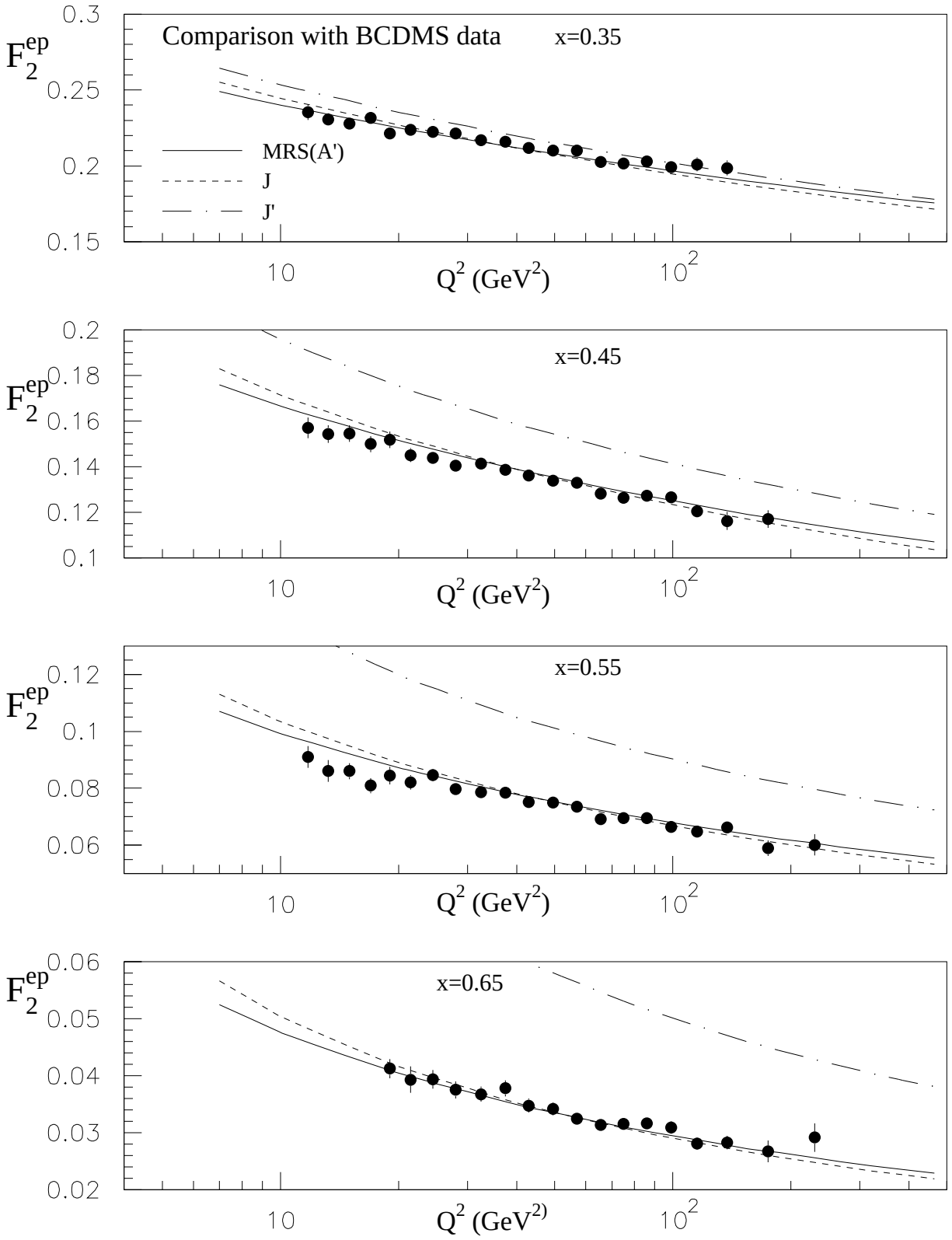
Comparison with BCDMS data
x=0.35
MRS(A')
J
J'
F_2^{ep}
Q^2 (GeV^2)
x=0.45
x=0.55
x=0.65
Q^2 (GeV$^{2)}$

Fig. 3

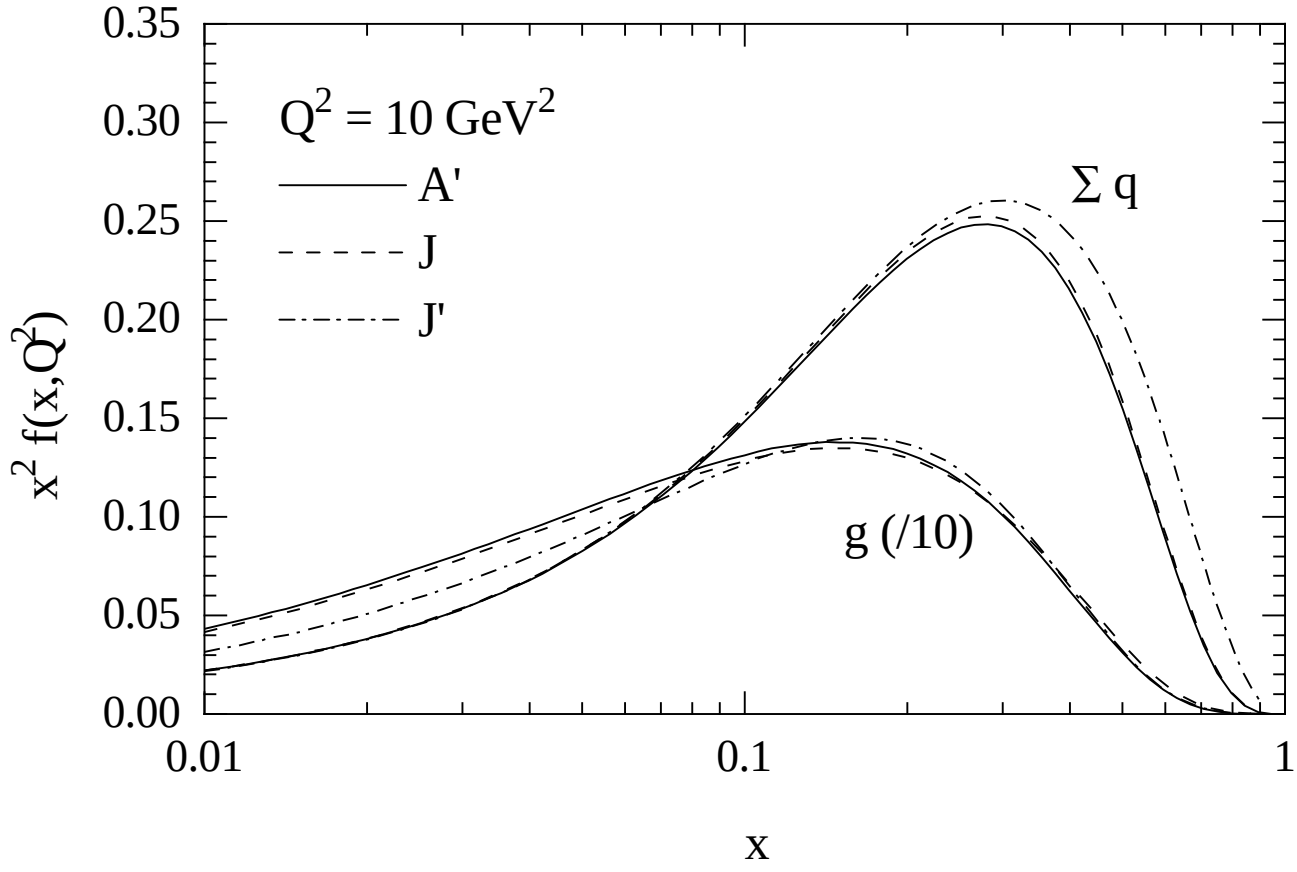
$Q^2 = 10\ GeV^2$
A'
J
J'
Σ q
g (/10)
$x^2\ f(x,Q^2)$
0.35
0.30
0.25
0.20
0.15
0.10
0.05
0.00
0.01
0.1
1
x

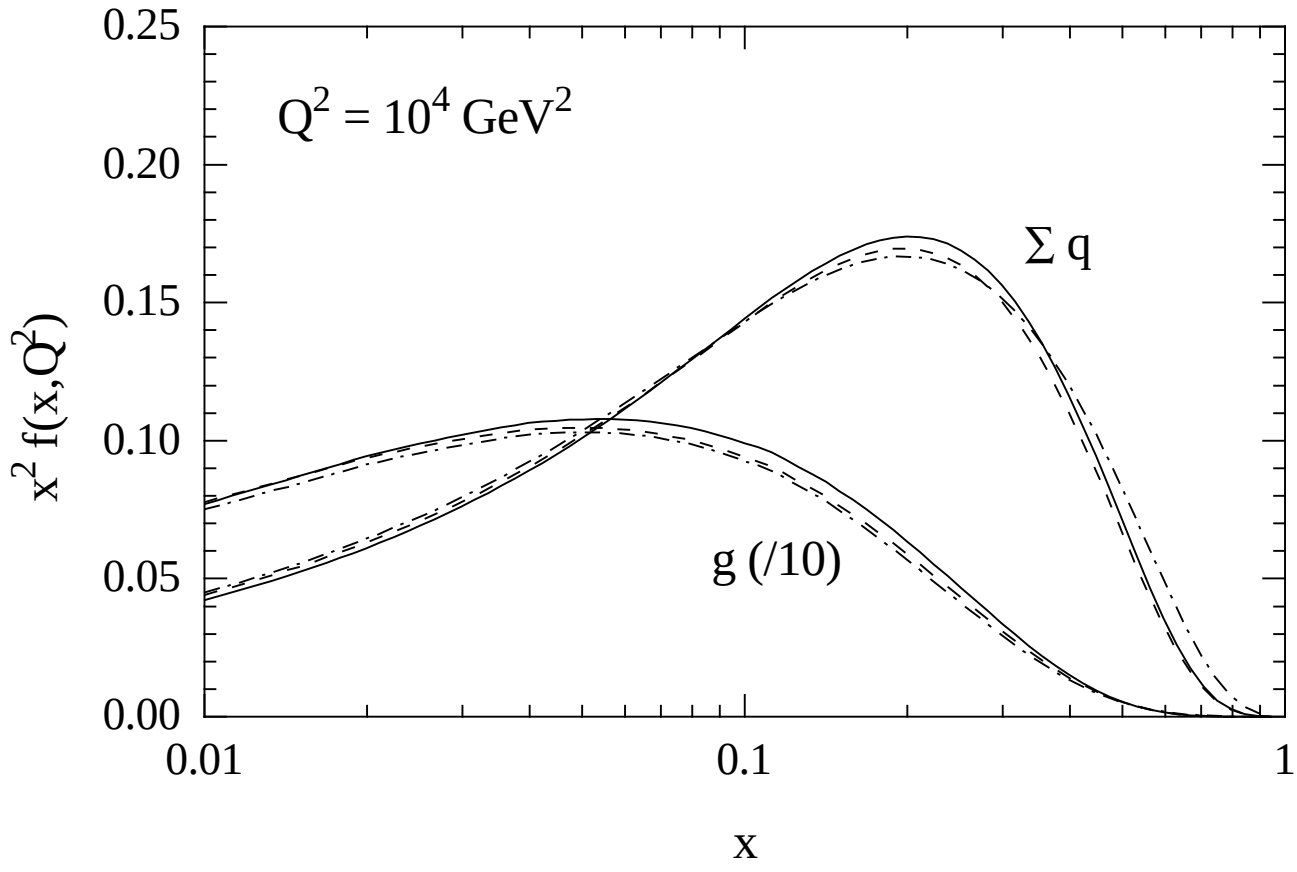
$Q^2 = 10^4\ GeV^2$
Σ q
g (/10)
$x^2\ f(x,Q^2)$
0.25
0.20
0.15
0.10
0.05
0.00
0.01
0.1
1
x

Fig. 4